MARS' NOACHIAN-HESPERIAN INTENSIVE FLUVIAL ACTIVITY DRIVEN BY ATMOSPHERIC COLLAPSE.

P. B. Buhler. Planetary Science Institute (pbuhler@psi.edu).

Introduction: Mars's surface was modified by liquid water flow in roughly three epochs: a modest Noachian (~>3.6 Ga) river-forming period, intensive Late Noachian-Early Hesperian (~3.6 Ga) valley-network-forming period, and later (~<3.5 Ga) localized flows [1-3]. The intensive valley network formation period is particularly enigmatic because it follows the less intense, earlier Noachian style of fluvial erosion [3], even though most processes (e.g., volcanism, impacts, thicker atmosphere) typically invoked to sustain surface water were waning by that time [1]. Climate models predict that most of Mars' water inventory was frozen in southern ice sheets at ~3.6 Ga [4], seemingly at odds with the emergence of an optimal period of fluvial erosion. However, I use numerical modeling to show that insulation from an extensive CO_2 ice sheet atop a south polar H_2O ice sheet [5] due to collapse of Mars' CO_2 atmosphere at ~3.6 Ga [6, 7] would trigger extensive basal ice sheet melting, leading to global-scale flooding and an attendant period of enhanced fluvial erosion (Fig. 1).

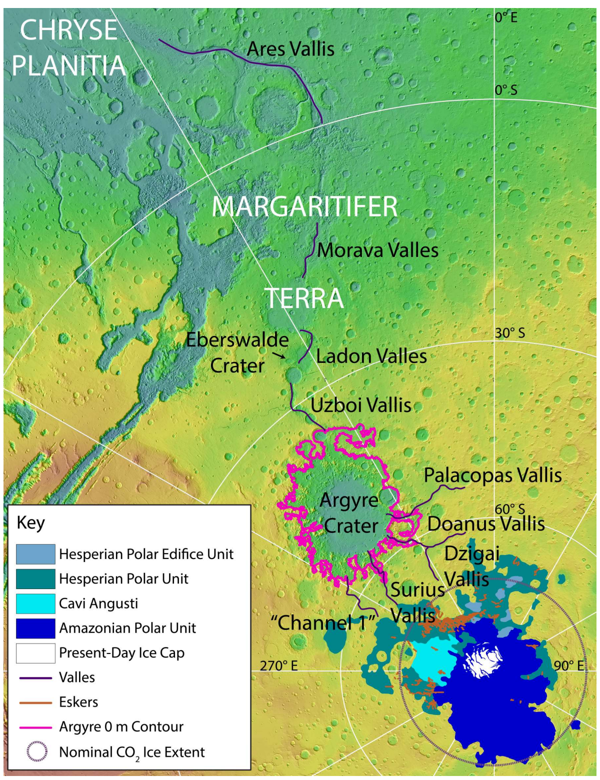

Fig. 1: MOLA [8] elevation map (blue, low = -5000 m; red, high = +6000 m) in Mars south polar projection. Map units from [9] and esker distribution from [10]. "Channel 1" is nomenclature from [11]. CO_2 ice sheet extent assumes nominal model parameters and constant 660 m depth.

Methods: A regolith adsorption and atmospheric equilibration model [12] is used to calculate the CO_2 ice cap mass $m_{CO_2,cap}$ collapsed on a pre-existing south polar H_2O ice cap [5]. Ice column thermal structure and H_2O basal melting is modeled using a 1-D thermal conduction scheme accounting for geothermal heat F_{geo} [13], strain heating in the H_2O ice, latent heats of sublimation and fusion, mass balance, the formation of structure-I CO_2 hydrate clathrate (a cage-like structure of H_2O enclosing CO_2 guest molecules), and glacial flow. The model has appropriate temperature bounds at the surface, base, and interface between ices and clathrate. Modeled collapse initiates at 30° obliquity from an inflated 600 mbar atmosphere to a collapsed pressure of 11 mbar at the CO_2 ice cap surface (set by vapor pressure equilibrium) in 10^4 yr [6, 7], accounting for CO_2 adsorbed in the regolith [12]. Collapse occurs onto the south pole, the favored location in Noachian climate models [4] and in the modern climate [14].

In the column model, CO_2 accumulates to thickness h_{CO_2}, set by the onset of basal CO_2 melting because model deposition far exceeds glacial flow subsidence. Clathrate forms at the CO_2-H_2O ice boundary, where it is thermodynamically favored. Column thermal profiles are calculated iteratively using temperature-dependent CO_2, H_2O, and clathrate thermal conductivities [15-17]. H_2O ice strain heating $F_{strain} = 2A_T\sigma^4$, with shear strain σ and empirical constant A_T ranged across low to high values from [18], is also calculated iteratively. Maximum H_2O ice column thickness h_{H_2O} is set by the onset of basal H_2O melting. Modeled bare H_2O ice column h_{H_2O} = 2-4 km, depending on assumed F_{geo}, so initial H_2O column thickness $h_{H_2O,init}$ is set to 2-4 km, consistent with prior 3-D models [5, 10]. Basal melt volume V_{melt} is calculated from the difference in $h_{H_2O,init}$ and h_{H_2O} after CO_2 deposition, multiplied by collapse area A_{CO_2}. Melt flux is calculated from available column heat flux and latent heat of H_2O melting once the basal temperature reaches the melt point. The model does not include the effects of dust, salts, H_2O basal sliding heating, or CO_2 strain or sliding heating—any of which would enhance H_2O basal melting.

Results: ***Atmospheric Collapse.*** Accounting for uncertainty in parameters relevant to regolith adsorption [12], $m_{CO_2,cap} = 3.4^{+0.8}_{-0.7} \times 10^{18}$ kg. Nominal h_{CO_2} = 660 m for 50 mW m^{-2} heat flux. Nominal $A_{CO_2} = 3.2^{+0.8}_{-0.6} \times 10^{12}$ m^2. Across all models, heat flux varies from ~45—100 mW m^{-2}, yielding a factor of ~3 variance in h_{CO_2} and A_{CO_2}.

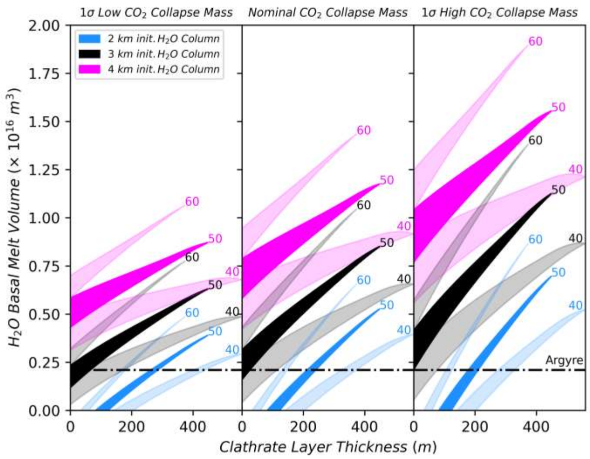

Fig. 2: Model-predicted volume of H_2O basal melt. Subpanels show low, nominal, and high CO_2 collapse mass models. Colors indicate $h_{H_2O,init}$. Shaded regions indicate melt range for F_{geo} = 40, 50, and 60 mW m^{-2} (labeled) bounded by assumptions of low and high shear heating. Argyre volume up to 0 m breach contour (pink in Fig. 1) provided for reference.

Water Melt Volumes and Flux. Model-predicted V_{melt} generally ranges from 10^{15}—10^{16} m^3 (Fig. 2), i.e., ~0.2 – 2.0 × Mars' present-day estimated global inventory or 4-40% of the likely maximum Late Noachian inventory [4]. V_{melt} increases with larger $h_{H_2O,init}$, more clathration, higher F_{geo}, and higher A_T. Model melt flux spans 3.3×10^2—3.0×10^3 m^3 s^{-1}, consistent with basal melt production estimated from Hesperian Polar Unit eskers [10, 11] (Fig. 1, 3). Collapse-triggered basal melting is also consistent with the lack of association between eskers and volcanic edifices [10]. For all model runs, complete column melt times are a few × 10^5 yr. Atmospheric collapse likely lasted ~10^4 – 10^7 yr, for collapse driven by a dip to low (<~30°) obliquity during a generally high obliquity state or entry into a persistently low (<~30°) obliquity state, respectively [19], so complete melting may or may not occur during a given collapse.

Discussion: Several 100s-km sinuous valleys leading from the Hesperian Polar Unit (Fig. 1) have been previously proposed to record melt water flow from a Noachian-Hesperian ice cap into a lake in Argyre Crater [11, 20]. Argyre paleolake has been proposed to have breached, sourcing flow into the Uzboi-Ladon-Marova system, and delivering water at least as far equatorward as Margaritifer Basin [21] (Fig. 1). Such delivery could potentially seeding a previously proposed cycle of Hesperian outflow megaflooding in Chryse Planitia [23]. Argyre overflow has been criticized primarily because no plausible mechanism for delivering sufficient water to cause breaching has previously been identified, although morphologic evidence is consistent with such an overflow [20]. Modeled V_{melt} indicates that polar basal melting triggered by atmospheric collapse could provide water sufficient for breaching (Fig. 2).

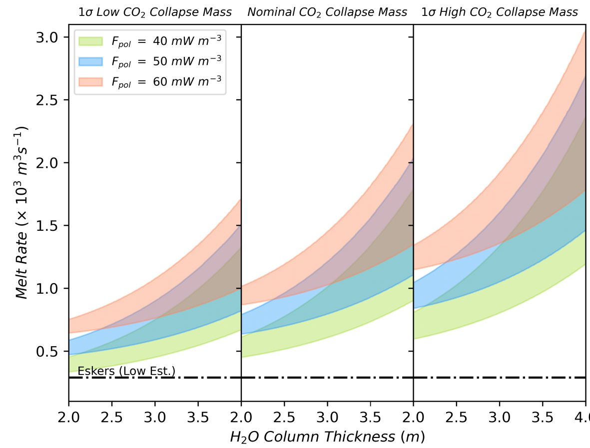

Fig. 3: Basal H_2O melt rate as a function of H_2O column thickness for various scenarios. Green, blue, and red regions indicate range of melting rates from low to high shear heating for F_{geo} = 40, 50, and 60 mW m^{-2}, respectively. Melt rate estimate from eskers [10] is provided for reference.

Conclusions: Water delivery from cyclic collapse events modeled here has timescales consistent with inferred valley network formation from episodic runoff over >~10^6 yr followed by abrupt cessation of fluvial activity [1]. Over ~10^8 yr, the effectiveness of polar basal melting would decrease due to the decline in Mars' volatile inventories [22] and F_{geo} [13]. These model results indicate that Mars' period of intensive fluvial activity near the Noachian-Hesperian boundary may have occurred in a collapsed-atmosphere climate similar to modern Mars, permitted principally by the formation of large CO_2 and H_2O polar deposits.

Acknowledgments: This work was supported by NASA Grant 80NSSC21K0212. **References:** [1] Fassett, C.I., Head, J.W., 2011. *Icarus* 211, 1204-1214. [2] Kite, E.S., 2019. *Space Sci Rev* 215, 10. [3] Irwin, R.P. et al., 2005. JGR *Planets*, 110(E12). [4] Fastook, J.L., Head, J.W., 2015. *PSS* 106, 82-98. [5] Fastook, J.L. et al., 2012. *Icarus* 219, 25-40. [6] Forget, F. et al., 2013. *Icarus* 222, 81-99. [7] Soto, A. et al., 2015. *Icarus* 250, 553-569. [8] Smith, D.E. et al., 1999. *Science* 284, 1495-1503. [9] Tanaka, K.L. et al.., 2014. *PSS* 95, 11-24. [10] Scanlon, K.E. et al., 2018. *Icarus* 299, 339-363. [11] Head, J.W., Pratt, S., 2001. *JGR Planets* 106(E6). [12] Buhler, P.B., Piqueux, S., 2021. *JGR Planets* 126, e2020JE006759. [13] Solomon, S.C. et al., 2005. *Science* 307, 1214-1220. [14] Buhler, P.B. et al., 2020. *Nat Astro* 4, 364-371. [15] Mellon, M.T., 1996. *Icarus* 124, 268-279. [16] Petrenko, V., Whitworth, R., 1999. *Oxford U Press*. [17] Jiang, H., Jordan, K.D. 2010. *J Phys Chem C* 114, 5555-5564. [18] Cuffey, K.M., Paterson, W.S.B. 2010. *Academic Press*, 223-284. [19] Laskar, J. et al., 2004. *Icarus* 170, 343-364. [20] Hiesinger, H., Head, J.W., 2002. *PSS* 50, 939-981. [21] Grant, J.A., Parker, T.J., 2002. *JGR Planets* 107, 4-1. [22] Jakosky, B.M., 2021. *Ann Rev Earth Plan Sci* 49, 71-93. [23] Moore, J.M., et al., 1995. *JGR Planets* 100, 5433-5447.